


Editorial

Editorial for Special Issue “New Discovery and Exploration Methods of Porphyry and Epithermal Mineral Deposits”

Chao Yang , Yiwei Peng * and Gangyang Zhang

College of Earth and Planetary Sciences, Chengdu University of Technology, Chengdu 610059, China; yangchao_21@126.com (C.Y.); zhanggangyang@163.com (G.Z.)

* Correspondence: yiwei_peng@163.com

1. Background and Scope of the Special Issue

Porphyry deposits and their genetically and spatially associated epithermal deposits constitute one of the most economically significant mineral systems, attracting extensive attention from both industrial practitioners and academic researchers. Widely targeted in mineral exploration and genetic studies, this deposit system ranks among the most thoroughly investigated ore deposit types. Nevertheless, new discoveries and novel advances in its metallogenic mechanisms and exploration techniques continue to emerge. These findings deepen our fundamental understanding of porphyry mineralization and facilitate the formulation of optimized exploration strategies for prospective mineral prospecting.

To disseminate cutting-edge achievements regarding the metallogeny and exploration methodologies of porphyry and epithermal deposits, and keep relevant professionals informed about the latest research developments, we launch this Special Issue to share updated research insights on these two major deposit types.

This collection of 16 studies included in the Special Issue systematically investigates the geology, geochemistry, mineralogy, geochronology, hydrothermal evolution, metallogenic mechanisms, exploration indicators, and magmatic origins of diverse porphyry, skarn, epithermal, and trans-porphyry ore deposits distributed across Xizang (Tibet, China), Xinjiang (China), northern China, Türkiye, Canada, Australia, Brazil, Siberia, Hungary and France. These papers apply multiple analytical methods, including zircon U-Pb and Hf isotopes, Re-Os dating, fluid inclusions, stable S/C/O isotopes, SWIR spectroscopy, whole-rock geochemistry, indicator mineral chemistry (zircon, apatite, titanite, and pyrite), sulfide microanalysis and statistical discrimination models; they reveal hydrothermal fluid evolution, magmatic redox conditions, fluid mixing/precipitation mechanisms, magmatic source properties, alteration zoning, granite fertility evaluation, and magma reservoir processes. Collectively, these papers provide a comprehensive understanding of the porphyry–skarn–epithermal metallogenic systems, caldera-related epithermal mineralization, Archean–Paleoproterozoic ancient porphyry metallogeny, regional exploration vectors, and a novel trans-porphyry Sn–Ta–Nb–gem deposit metallogenic model, thus fulfilling the Special Issue’s objective of disseminating cutting-edge progress in the field.

2. Individual Contributions of Each Paper

Vignerresse (2026) (Contribution 1) proposes a novel trans-porphyry deposit (TPD) metallogenic theory that is distinct from traditional subduction porphyry deposits, revealing low-crustal melting mechanisms for Sn-Ta-Nb-gem mineralization during large-scale shear between cratons within continental plates, internal decoupling, and vertical motion. The



Received: 14 May 2026

Accepted: 25 May 2026

Published: 2 June 2026

Copyright: © 2026 by the authors. Licensee MDPI, Basel, Switzerland. This article is an open access article distributed under the terms and conditions of the [Creative Commons Attribution \(CC BY\) license](https://creativecommons.org/licenses/by/4.0/).

study differentiates the formation processes of NYF/LCT pegmatites and gem minerals, providing new insights into porphyry-related deposit diversity for the Special Issue.

Guan et al. (2025) (Contribution 2) identify four pyrite types that record successive hydrothermal stages of the Zhunuo porphyry Cu deposit in Xizang, using LA-ICP-MS pyrite mineral geochemical data to reveal trace-element coupling behaviors and oxygen fugacity fluctuations during hydrothermal evolution. The study also establishes pyrite trace-element proxies and PLS-DA discrimination indicators, which effectively distinguish porphyry–epithermal systems on the Tibetan Plateau and contribute to the Special Issue’s focus on hydrothermal processes and exploration indicator minerals.

Cheng et al. (2025) (Contribution 3) determine the petrogenesis of the Late Carboniferous subduction-related granites in the Baijianshan skarn Zn-Cu deposit via zircon U-Pb-Hf isotopes, whole rock geochemistry, and fluid inclusion characteristics. They clarify that the granites were derived from the juvenile crystal and formed in a subduction-related back basin, and ore-forming fluids originated from the mixing of magmatic and meteoric water. The research also confirms that the deposit forms a unified skarn–epithermal metallogenic system with adjacent epithermal deposits, advancing understanding of the correlation between skarn and epithermal systems highlighted in the Special Issue.

Kocatürk et al. (2025) (Contribution 4) characterizes multistage magmatic redox evolution and the continuous porphyry–skarn transition in the Eocene Tavşanlı Belt of Türkiye using whole-rock geochemistry, amphibole–biotite chemistry, and molybdenite Re-Os dating. The study constructs a unified syn–post-subduction genetic model for spatially associated Cu-Mo-W-Au mineralized systems, enriching the Special Issue’s content on the metallogeny of porphyry-related deposits.

Hong et al. (2025) (Contribution 5) classify two types of early Oligocene ultrapotassic lamprophyre dykes in the Bangbule area of Xizang, constraining their lithospheric mantle source metasomatized by Indian continental crust melts through Sr-Nd isotopic analysis. The research proposes an open magma chamber model featuring fractional crystallization and mafic magma recharge, providing key insights into magmatic processes relevant to porphyry deposit formation.

Zhou et al. (2025) (Contribution 6) conduct in situ geochemical analysis of garnet and cassiterite from the Gongjuelong skarn Sn deposit, distinguishing the physicochemical conditions of different skarn stages. The study demonstrates that proximal skarn Sn and distal hydrothermal Pb-Zn-Ag deposits form an integrated granite-related metallogenic system in the Yidun Terrane, related to the late Cretaceous highly fractionated granites. This research proposed hypothesis highlights the potential prospecting of Sn mineralization beneath the hydrothermal Pb-Zn-Ag veins, aligning with the Special Issue’s focus on deposit genesis and new exploration prospects.

Katz et al. (2025) (Contribution 7) systematically analyze the alteration lithochemistry and mass balance changes in the world-class Archean Côté Au(-Cu) porphyry deposit in Canada, defining zoned metal element assemblages and hydrothermal alteration footprints. The research further verifies the porphyry-type genetic model for this Archean gold system, contributing to the Special Issue’s exploration of ancient porphyry deposits.

Quan et al. (2025) (Contribution 8) obtain systematic S/C/O isotope data of sulfides and carbonates from the Permian Drake epithermal Au-Ag field in Australia, revealing multiple mixed sources of ore-forming fluids and sulfur. The study clarifies metallogenic mechanisms in collapsed volcanic caldera settings, optimizing epithermal exploration strategies and addressing the Special Issue’s focus on epithermal deposit exploration.

Li et al. (2025) (Contribution 9) integrate SWIR spectroscopy, EPMA, and XRD to study hydrothermal alteration minerals in the Sinongduo low-sulfidation epithermal deposit in the Gangdese belt of Xizang, establishing spatial alteration mineral zoning and white

mica SWIR exploration models. The research predicts high mineralization potential in the northern Woruo area, advancing spectroscopy-based exploration methods highlighted in the Special Issue.

Wang et al. (2025) (Contribution 10) analyze muscovite SWIR spectral parameters (Al-OH wavelength and crystallinity) of the Yixingzhai gold deposit in Shanxi, revealing distinct spectral differences among porphyry, quartz vein, and breccia mineralization types. The study proposes muscovite crystallinity as a key indicator for porphyry gold exploration, enriching the Special Issue's content on exploration indicators.

Lee et al. (2025) (Contribution 11) conduct detailed geochronology and petrology on the Late Cretaceous porphyry and epithermal deposit in Canada's Dawson Range gold belt, identifying two newly recognized causative magmatic suites linked to Au mineralization. The research reveals a tectonic transition from subduction to local extension that controls regional porphyry belt metallogeny, contributing to the Special Issue's focus on geochronology and regional metallogeny.

Crépon et al. (2024) (Contribution 12) confirm the Neoproterozoic Chibougamau pluton hosts typical porphyry-type Cu-Au mineralization via whole-rock geochemistry, zircon chemistry, and fluid inclusion data. The study clarifies that moderately oxidized intermediate magmas provide metalliferous fluids, establishing an Archean porphyry metallogenic genetic model and expanding the Special Issue's coverage of ancient porphyry systems.

Lopes et al. (2024) (Contribution 13) constrain the hydrothermal conditions, fluid sources, and gold precipitation mechanisms of the Paleoproterozoic Raimunda porphyry Au deposit in Brazil's Amazonian Craton using fluid inclusion and stable isotope data. The research provides important prospecting implications for ancient Amazonia cratonic porphyry gold systems, supporting the Special Issue's exploration focus.

Berzin et al. (2024) (Contribution 14) evaluate granite metallogenic fertility in Siberia's Taimyr Peninsula using zircon, apatite, and titanite indicator minerals plus whole-rock geochemistry. The study identifies oxidized water-saturated fertile granitoid intrusions favorable for Cu-Mo mineralization and grades regional exploration targets, addressing the Special Issue's focus on indicator minerals and exploration strategies.

Biró et al. (2024) (Contribution 15) perform a comparative sulfide compositional study on porphyry, skarn, and carbonate-replacement mineralization in Hungary's Recsk complex, establishing distinctive trace-element geochemical fingerprints for each mineralization type. The research proposes sulfide trace-element evolutionary trends as effective hydrothermal system vectoring tools, contributing to geochemical exploration methods in the Special Issue.

Gao et al. (2024) (Contribution 16) systematically summarize the geological, geochemical, and geophysical characteristics of the Luming porphyry Mo deposit in NE China, revealing that hydrothermal breccias control mineralization and form distinct metal primary halo zoning. The study confirms the deposit belongs to a complete porphyry-skarn-epithermal system, providing regional prospecting guidance and aligning with the Special Issue's exploration and metallogeny focus.

Acknowledgments: The Guest Editors thank the authors, reviewers, and the Editorial Board, as well as the staff from *Minerals*, for their contributions to this Special Issue.

Conflicts of Interest: The authors declare no conflicts of interest.

List of Contributions

1. Vigneresse, J.-L. Specificity of Ore Generation (Tin, Pegmatites, and Gems) in Trans-Porphyry Deposits. *Minerals* **2026**, *16*, 157. <https://doi.org/10.3390/min16020157>.
2. Guan, H.; Luosang, J.; Gao, L.; Xie, F. Pyrite Trace-Element Signatures of Porphyry-Epithermal Systems in Xizang: Implications for Metallogenic Discrimination and Hydrothermal Evolution. *Minerals* **2025**, *15*, 1113. <https://doi.org/10.3390/min15111113>.

3. Cheng, F.; Zhang, S.; Wu, J.; Huang, B.; Zhang, D. Genesis of the Baijianshan Skarn-Type Zn-Cu Polymetallic Deposit, Chinese Eastern Tianshan: Constraints from Geology, Geochronology and Geochemistry. *Minerals* **2025**, *15*, 1107. <https://doi.org/10.3390/min15111107>.
4. Kocatürk, H.; Kumral, M.; Sendir, H.; Kaya, M.; Creaser, R.A.; Abdelnasser, A. Magmatic Redox Evolution and Porphyry–Skarn Transition in Multiphase Cu-Mo-W-Au Systems of the Eocene Tavşanlı Belt, NW Türkiye. *Minerals* **2025**, *15*, 792. <https://doi.org/10.3390/min15080792>.
5. Hong, C.; Wang, Y.; Zunzhu, S.; He, C.; Wang, H.; Wang, Y.; Bai, Y.; Yan, P.; Xun, S.; Cao, R.; et al. Mineralogy and Petrology of Ultrapotassic Lamprophyre Dykes in the Bangbule Area, Xizang, China: Evidence for Open Magma Chamber Fractionation and Mafic Magma Recharge. *Minerals* **2025**, *15*, 332. <https://doi.org/10.3390/min15040332>.
6. Zhou, Y.; Peng, Y.; Liu, C.; Tian, J.; Wang, Z.; Song, M.; Zhang, Y. Genesis of the Gongjuelong Sn Polymetallic Deposit in the Yidun Terrane, China: Constraints from the In Situ Geochemistry of Garnet, Cassiterite, and Quartz. *Minerals* **2025**, *15*, 314. <https://doi.org/10.3390/min15030314>.
7. Katz, L.R.; Kontak, D.J.; Dubé, B. Alteration Lithochemistry of an Archean Porphyry-Type Au(-Cu) Setting: The World-Class Côté Gold Deposit, Canada. *Minerals* **2025**, *15*, 256. <https://doi.org/10.3390/min15030256>.
8. Quan, H.; Graham, I.; Worland, R.; Adler, L.; Dietz, C.; Madayag, E.; Wang, H.; French, D. Interpreting the Complexity of Sulfur, Carbon, and Oxygen Isotopes from Sulfides and Carbonates in a Precious Metal Epithermal Field: Insights from the Permian Drake Epithermal Au-Ag Field of Northern New South Wales, Australia. *Minerals* **2025**, *15*, 134. <https://doi.org/10.3390/min15020134>.
9. Li, X.; Guo, N.; Li, C.; Deng, S.; Zhou, W. Shortwave Infrared Spectroscopy and Geochemical Characteristics of White Mica-Group Minerals in the Sinongduo Low-Sulfide Epithermal Deposit, Tibet, China. *Minerals* **2025**, *15*, 104. <https://doi.org/10.3390/min15020104>.
10. Wang, L.; Wu, S.; Lai, X.; Yang, W.; Sun, R.; Liu, P.; Yang, Y.; Ren, Y. The Short-Wave Infrared (SWIR) Spectral Exploration Identification and Indicative Significance of the Yixingzhai Gold Deposit, Shanxi Province. *Minerals* **2025**, *15*, 83. <https://doi.org/10.3390/min15010083>.
11. Lee, W.-S.; Kontak, D.J.; Sack, P.J.; Crowley, J.L.; Creaser, R.A. Geology, Petrology and Geochronology of the Late Cretaceous Klaza Epithermal Deposit: A Window into the Petrogenesis of an Emerging Porphyry Belt in the Dawson Range, Yukon, Canada. *Minerals* **2025**, *15*, 38. <https://doi.org/10.3390/min15010038>.
12. Crépon, A.; Mathieu, L.; Kontak, D.J.; Marsh, J.; Hamilton, M.A. An Archean Porphyry-Type Deposit: Cu-Au Mineralization Associated with the Chibougamau Tonalite–Diorite Pluton, Abitibi Greenstone Belt, Canada. *Minerals* **2024**, *14*, 1293. <https://doi.org/10.3390/min14121293>.
13. Lopes, A.A.C.; Moura, M.A. The Paleoproterozoic Raimunda Porphyry-Type Gold Deposit, Juarena Mineral Province, Amazonian Craton (Brazil): Constraints Based on Petrological, Fluid Inclusion and Stable Isotope Data. *Minerals* **2024**, *14*, 1185. <https://doi.org/10.3390/min14121185>.
14. Berzin, S.V.; Konopelko, D.L.; Petrov, S.V.; Proskurnin, V.F.; Berzon, E.I.; Kurapov, M.Y.; Golovina, T.A.; Chernenko, N.Y.; Chervyakovskiy, V.S.; Palamarchuk, R.S.; et al. Evaluation of Granite Fertility Utilizing Porphyry Indicator Minerals (Zircon, Apatite, and Titanite) and Geochemical Data: A Case Study from an Emerging Metallogenic Province in the Taimyr Peninsula, Siberian High Arctic. *Minerals* **2024**, *14*, 1065. <https://doi.org/10.3390/min14111065>.
15. Biró, M.; Raith, J.G.; Feichter, M.; Hencz, M.; Kiss, G.B.; Virág, A.; Molnár, F. Comparative Study of Sulfides from Porphyry, Skarn, and Carbonate-Replacement Mineralization at the Recsk Porphyry-Mineralized Complex, Hungary. *Minerals* **2024**, *14*, 956. <https://doi.org/10.3390/min14090956>.
16. Gao, B.; Dong, M.; Xie, H.; Liu, Z.; Li, Y.; Zhou, T. Discovery and Exploration of the Luming Porphyry Mo Deposit, Northeastern China: Implications for Regional Prospecting. *Minerals* **2024**, *14*, 718. <https://doi.org/10.3390/min14070718>.

Disclaimer/Publisher’s Note: The statements, opinions and data contained in all publications are solely those of the individual author(s) and contributor(s) and not of MDPI and/or the editor(s). MDPI and/or the editor(s) disclaim responsibility for any injury to people or property resulting from any ideas, methods, instructions or products referred to in the content.